SCIENTIFIC REPORTS

OPEN

Cerium oxide nanoparticles embedded thin-film nanocomposite nanofiltration membrane for water treatment

Sonia R. Lakhotia[1,2], Mausumi Mukhopadhyay[2] & Premlata Kumari[1]

In this paper, a new approach to synthesize thin-film nanocomposite membranes using cerium oxide (CeO_2) nanoparticles (NPs) by pre-seeding interfacial polymerization method was reported. Prepared membranes were examined using contact angle, molecular weight cut-off (MWCO), scanning electron microscopy (SEM), Fourier transform infrared spectroscopy (FTIR) and scanning probe microscopy (SPM) to observe its hydrophilicity, pore size, morphology, surface chemistry, and roughness, respectively. Surface charges of the prepared membranes were also qualitatively calculated with the help of contact angle measurements by using the Grahame equation. MWCO studies revealed >90% polyethylene glycol (M.W. 1500 Da) rejection, which was fitted in the range of nanofiltration. By increasing the concentration of CeO_2 NPs, flux (33.12 to 41.28 L/m²h), hydrophilicity (77.3 to 51.1°) and surface charges (-7.58 to -13.39 mC/m²) of the membranes was successfully improved, and also showed the high (>90%) salt rejections. The CeO_2 embedded membrane was also found out in successful prevention from the attack of bacteria (*Escherichia coli*) compared to pure polyamide (PA) membrane and confirmed through SEM and viable cell count method. The membrane performances were also evaluated using seawater for fouling study and found that CeO_2 embedded surface increased the rejection of hydrophobic contaminants, and notably reduced the fouling.

The scarcity of clean water along with the increasing contamination of river bodies is one of the most severe problems faced worldwide[1,2]. Conventional water filtration technique is energy consuming processes and also fails to fulfill all the requirements of human beings. Thus developing effective water treatment approaches is one of the most indispensable needs of the hour[3]. Nowadays membrane separation technique has gained a significant role in separation and purification of water as they are eco-friendly and faster. Nanofiltration (NF) membrane is one of the largely used separation technique[4,5] especially in desalination and various industrial applications[6] for the production of clean and safe water. However, polymeric membranes are not efficient due to its low stability with limited life durability, selectivity, and hydrophobic nature[7–9]. Hydrophobic nature of membrane causes severe fouling especially bio-fouling causing a decline in the separation efficiency and flux in water treatment. Several methods have been considered in order to reduce fouling[6]. Therefore at the present time, nanocomposite membrane prepared by embedding nanomaterials is gaining a great importance in the field of membrane separation for water treatment[10]. The recent study has been focused on low-cost, durable anti-fouling nanocomposite membrane for the water treatment. These nanoparticles (NPs) embedded membranes are control over polymeric membrane[11] as it can be easily tailored as per the conditions of separation with improved smoothness, stability, hydrophilicity, and antibacterial activity[12,13].

In past years, various NPs like TiO_2[6,14,15], zeolite[16–18], and silica[5,19] have been used for the preparation of nanocomposite membrane which shows enhanced flux, fouling-resistant, and salt rejection properties. But comparing with different types of fouling, bio-fouling is a bigger problem in the application of NF membrane[2,15] in which bacteria grow on the membrane surface during the separation process. Due to their self-reproducing nature, it is very difficult to maintain the efficiency of membrane separation. Silver[20–22], carbon nanotubes (CNTs)[20,23] and

[1]Applied Chemistry Department, Sardar Vallabhbhai National Institute of Technology, Surat, 395007, Gujarat, India. [2]Department of Chemical Engineering, Sardar Vallabhbhai National Institute of Technology, Surat, 395007, Gujarat, India. Correspondence and requests for materials should be addressed to M.M. (email: mausumi_mukhopadhyay@yahoo.com)

graphene oxide (GO)[24] NPs are the most considered nanofillers source that acts as an anti-bacterial agent to prevent bio-fouling from the membrane. Even though these NPs are very effective, but are expensive and not easily available. Hence exploration of such material that has anti-biofouling properties is very necessary. Copper (Cu) NPs is to be considered as an antibacterial material against various microorganisms including viruses, bacteria, and fungi[25]. But, its major drawback is its stability and can be easily aggregated, which can decrease its antibacterial activity.

In particular, cerium oxide (CeO$_2$) NPs have found great potential applications as nanofiller due to its low cost, high surface area and quick transformation between Ce^{+3} ↔ Ce^{+4} which enhance its antioxidant properties[26–28]. CeO$_2$ NPs is an effective biocide against various bacterial strains[26] and used in many known applications such as catalysis, sensors, purifying contaminated water and also in various industrial applications[27]. Still, only limited work has been reported and available on antibacterial activity in water treatment process with CeO$_2$ NPs. Pelletier et al. and Thill et al. have been reported antimicrobial activity of CeO$_2$ NPs against *Escherichia coli (E. coli)*[29,30], whereas Fang et al. have shown the antibacterial activity against *Nitrosomonas europaea*[31]. The colony forming units (CFU) after contact with CeO$_2$ NPs is lethal to bacteria. Peng et al. and his co-workers have been used CeO$_2$ supported CNTs composite adsorbent to study the adsorption capacity of arsenate from the potable water[32]. Authors observed that the prepared composite material (CeO$_2$-CNTs) have a great potential in removing arsenate efficiently compared to only CNTs due to its high electrostatic attraction between CeO$_2$-CNTs and arsenic (V) anions. The electrostatic attraction can facilitate and improve the adsorption of arsenic (V)[32]. Composites of CeO$_2$ NPs on CNTs are also used to adsorb the chromium (VI) ion from drinking water[33]. Therefore, CeO$_2$ NPs are expected to be suitable NPs as filler in the preparation of nanocomposite membrane.

There are two methods for preparing nanocomposite membrane: (i) coating and (ii) blending. The coating of NPs like TiO$_2$, zeolite, silica, CNTs, silver, GO has been widely used and is an easy way to modify the membranes[34–36]. The literature studies show that coating method involves a thin-film layer formation with NPs on a porous support without a major change in the membrane structure and morphology. Polysulfone (PS)[3] and polyethersulfone (PES)[2] have been commonly used as a porous support in the water filtration process because they have high strength and tunable pore size chemistry. Rahimpour et al. have discussed the comparison between membrane preparation by depositing and blending of NPs method. Authors found that the coating of NPs provides high surface layer sustainability by generating stronger physical/chemical bonds as compared to blending and also effectively improve the membrane performance[10] and it's anti-fouling ability.

By considering the advantages of CeO$_2$ NPs, in this work, CeO$_2$ NPs embedded thin-film nanocomposite (TFN) membranes are prepared on PES porous support by pre-seeding interfacial polymerization method and analyzed by molecular weight cut-off (MWCO), contact angle, scanning electron microscopy (SEM), attenuated total reflection (ATR) attached with Fourier transform infrared (FTIR) spectroscopy, transmission electron microscopy (TEM) and scanning probe microscopy (SPM). The TFN CeO$_2$ membrane performance is also evaluated using a cross-flow filtration setup for rejection performance (with different salt solution) and anti-fouling study using saltwater (seawater) collected from Suvali beach, Surat, India. In addition to this work, an antibacterial activity of this TFN membrane was also checked with *E. coli*. strain.

Results and Discussion

Membrane preparation.
Selection of an appropriate method for incorporating the particular NPs onto the membrane surface is as important as that of choosing the right NPs. There are two methods for embedding NPs into the polyamide (PA) thin-film membrane viz. conventional and pre-seeding polymerization[37,38]. Conventional methods are of two types depending on, whether the NPs are dispersed in m-phenylenediamine (MPD) or trimesoyl chloride (TMC) solution. If NPs are dispersed in TMC, an interfacial polymerization (IP) zone is formed below the NPs. Since the NPs are on the top most layers of the membrane it gets agglomerated and also has a great chance of leaching. If NPs are dispersed in MPD solution, IP zone is formed above the NPs followed by the formation of PA layer. Since the PA layer is on the top, fouling will be more[37]. To overcome this problem, an intermediate pre-seeding hexane solution containing a low concentration of TMC, ethanol, and NPs is introduced between MPD and TMC solution to assist the dispersion of NPs on the top surface of the membrane support. This resulted in the formation of an IP zone at the same layer (neither above nor below the NPs) of the membrane where the NPs are present (Fig. S1). Here, the PA layer is formed with the embedded NPs. Since a good bonding between the NPs and PA layer exists, problems like agglomeration and leaching of the NPs, fouling etc. are rectified. Thus to prepare self-cleaning and defect-free TFN NF membrane, pre-seeding interfacial polymerization by ultrasonication and stirring method is used to promote the proper dispersion of CeO$_2$ NPs within the PA layer (Fig. 1).

In this method, CeO$_2$ NPs (X-ray diffraction spectra of the available CeO$_2$ NPs shown in Fig. S2) hybrid NF membranes were prepared as 0-M1, 0.05-M2, 0.1-M3, 0.2-M4 and 0.3-M5. First, the aqueous liquid of sodium lauryl sulfate 0.15% (w/v) and MPD 2% (w/v) is slowly poured onto the PES support. After approximately 3 min, MPD dipped membranes are put on a sheet and moved with a roller to remove excess MPD solution. Then, a particular amount of CeO$_2$ NPs are dispersed in an organic phase of hexane, TMC and ethanol solution, separately, and subjected to sonication and stirring, where CeO$_2$ NPs are coordinately attached with the carbonyl group of TMC to form well dispersed pre-assembled CeO$_2$ NPs. CeO$_2$ NPs present in the solution (w/v) are 0% (0-M1), 0.05% (0.05-M2), 0.1% (0.1-M3), 0.2% (0.2-M4) and 0.3% (0.3-M5) respectively. This well dispersed sonicated solution is spread on MPD coated PES support membrane. This pre-assembled CeO$_2$ NPs forms IP zone at the same surface where the CeO$_2$ NPs are present and formed the PA layer with the CeO$_2$ NPs. After the evaporation of excess solution, 0.1% (w/v) organic solution of TMC is immediately poured, followed by 1 min polymerization reaction and then, rinsed with pure water and characterized by further study.
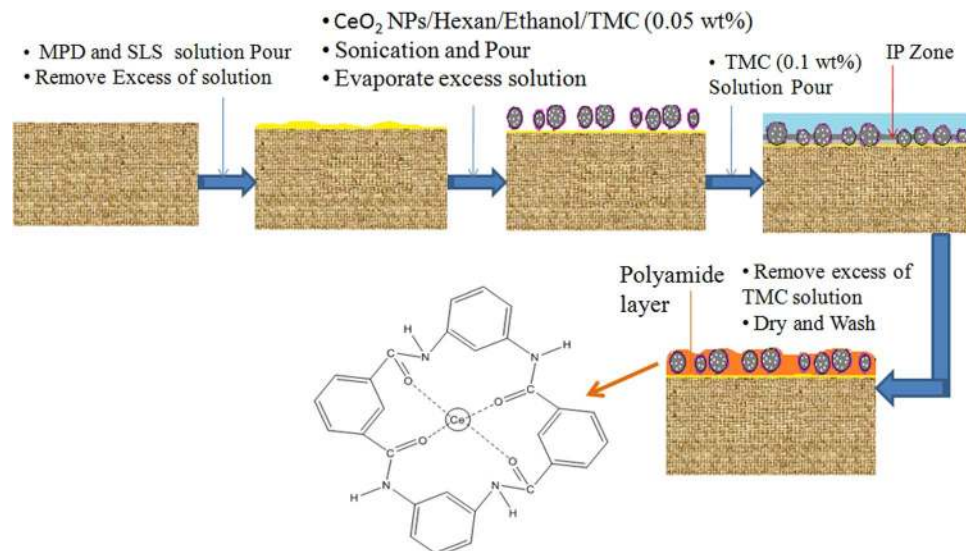
Figure 1. Steps of pre-seeding interfacial polymerization method for CeO$_2$ NPs embedded TFN membrane.

| Membranes	Contact angle (°)	Surface charge, mC/m^2 (at pH 7.0)	PEG (1500 Da) rejection %
0-M1	77.3	−7.58	88.77
0.05-M2	65.3	−10.78	89.09
0.1-M3	58.4	−12.21	90.33
0.2-M4	53.1	−13.34	90.86
0.3-M5	51.1	−13.39	92.11

Table 1. Pure water contact angles, surface charge and MWCO of the membranes.

Surface study and pore size.   Porous PES support can be covered with an increasing concentration of CeO$_2$ NPs, which increases the hydrophilicity, surface charge and MWCO of the CeO$_2$-PA TFN membrane and the results are shown in Table 1. More spreading of water, lesser the angle and the surface is more hydrophilic. The increase in hydrophilicity is due to the formation of nanovoids around the interface of CeO$_2$ NPs and PA layer, which directly affects the water uptake and diffusivity of the CeO$_2$-PA TFN membrane. The surface charge of the PA layer coated (0-M1) membrane is −7.58 mC/m^2. That is closer to the results of other researchers, where the value is −7.2 mC/m^2 at 7.0 pH[4]. With increasing CeO$_2$ NPs concentration, the surface charge improves up to −13.39 mC/m^2. Highly negatively charged CeO$_2$-PA TFN membrane is not attracted the natural foulants (negatively charged substances), thus shows its increased anti-fouling ability impart by embedded CeO$_2$ NPs. Moreover, MWCO of the prepared CeO$_2$-PA TFN membranes is studied by the rejection performance of polyethylene glycol (PEG) with different molecular weights (600, 1000, 1500 Da) (Table S1). Prepared CeO$_2$-PA TFN membranes show around 90% rejections with PEG 1500 Da, which is in the range of NF.

Surface morphology.   The surface roughness and morphologies of the prepared CeO$_2$-PA TFN membrane are analyzed by contact mode SPM and SEM (Fig. 2) analysis.
    SPM analysis quantifies the surface quality (either smooth or rough) of the membrane. This is an important estimation for the membrane's anti-fouling study. A membrane with low roughness has possessed a stronger anti-fouling and anti-bio-fouling activity. Here, the CeO$_2$ NPs are embedded in the PA layer that changes the surface roughness. The surface roughness of membrane decreases with increasing the concentration of CeO$_2$ NPs. Increase in CeO$_2$ NPs concentration reveals proper dispersion and distribution of NPs with the thin covering of TMC monomer layer on the surface. This tends to have increased the smoothness of the surface compared to control membrane. The roughness of PA membrane is 8.48 nm (0-M1, Fig. 2a). After deposition of CeO$_2$ NPs, the CeO$_2$-PA TFN membrane surface becomes smoother with 7.28 nm (0.05-M2, Fig. 2b), 4.79 nm (0.1-M3) and 2.02 nm roughness (0.2-M4, Fig. 2c), because the surface is totally covered by the proper dispersion and distribution of CeO$_2$ NPs embedded PA layer. This type of nanopattern arranged surface (smoother surface) based on PA layer removes the foulants from the surface by simply rinsing with water.
    SEM analysis observes the morphology of the membrane surface. Fig. 2e shows the seed-like surface morphology by embedding CeO$_2$ NPs compared with flaky structure (Fig. 2d) visible on the surface of PA layer coated membrane (0-M1). SEM (0.2-M4, Fig. 2e), reveals reasonably good dispersion of CeO$_2$ NPs that are attributed to the covering of thin layer on the surface of CeO$_2$ NPs (Fig. 2e). This covering provides the stable attachment of CeO$_2$ NPs on the CeO$_2$-PA TFN membrane surface, which is confirmed by the cross-sectional view (Fig. 2f),
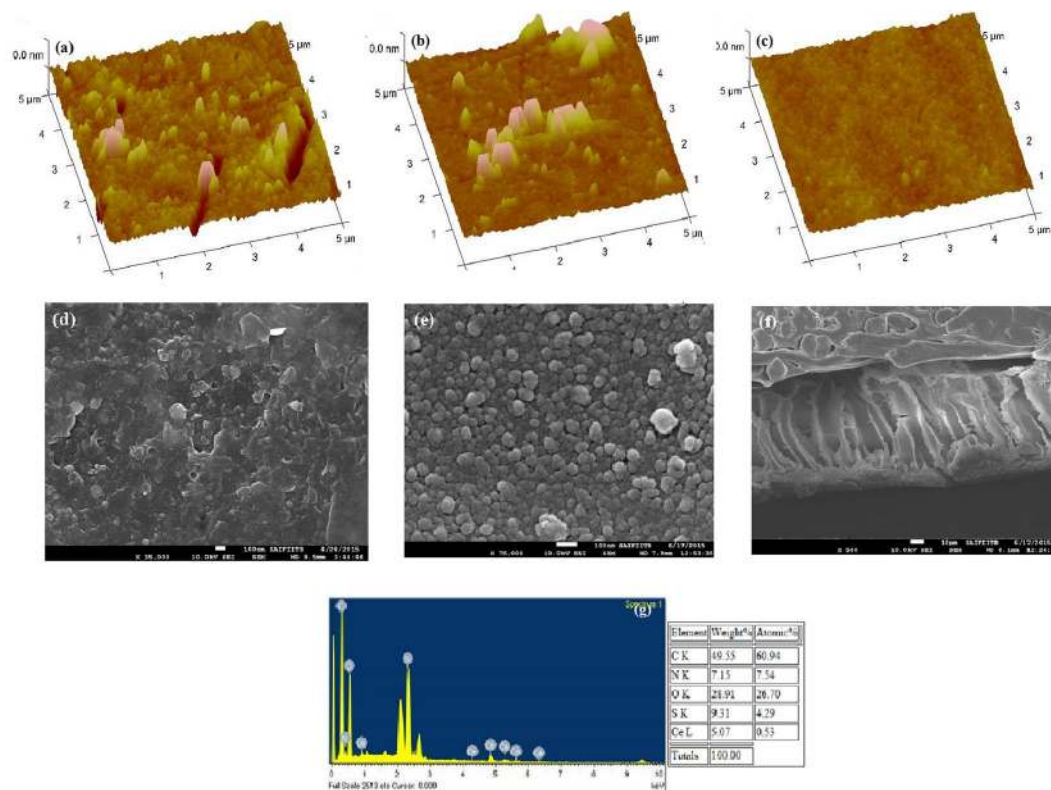
Figure 2. 3D SPM and SEM morphology of membranes: SPM images (**a**) 0-M1, (**b**) 0.05-M2 and (**c**) 0.2-M4 and SEM images (**d**) 0-M1 (**e**) 0.2-M4 (**f**) 0.2-M4 cross-section image and (**g**) 0.2-M4 EDS analysis.

| Membranes	Mechanical properties	
	Tensile strength (MPa)	Elongation (%)
PES support	5.0	0.04
0-M1	13.2	4.31
0.05-M2	25.6	7.42
0.1-M3	30.8	10.33
0.2-M4	45.2	14.18
0.3-M5	39.3	13.68

Table 2. Mechanical properties of the membranes.

and its cross-sectional EDS analysis (Fig. 2g). The TEM analysis of PA membrane (0-M1) and CeO_2 NPs embedded (0.2-M4) membrane, shown in the Fig. S3.

Surface composition.   The surface chemical vibrations of the prepared membrane are observed by the ATR-FTIR spectroscopy (Fig. S4). The peak at 1665 cm^{-1} can be credited to the amide I band, C–N and C=O stretching vibrations. A peak at 1608 cm^{-1} is due to aromatic amide [C C ring] breathing as well as N–H deformation vibration and 1243 cm^{-1} for C–N peak of the amide group. The intensity of C=O and C–N stretching is increased with increasing the concentration of CeO_2 NPs (Fig. 1). The peak at 1541 cm^{-1} can be credited to N–C stretching and N–H bending of –CO–NH– group.

Mechanical properties.   The mechanical strength and elongation properties of modified membranes are shown in Table 2. The tensile strength of the PES support membrane is 5.0 MPa. This is closer to the results of other researchers, where the value is 5.3 MPa. Table 2 represents the effect of the content of CeO_2 NPs on mechanical properties of the modified nanocomposite membrane. The elongation is 14.18% and tensile strength of membrane is 45.2 MPa when the optimal content of CeO_2 NPs 0.2 (0.2-M4) in the membrane. The results show that mechanical properties of the membrane are improved with the addition of CeO_2 NPs. The IP zone is formed by the cross-linked network between MPD, CeO_2 NPs, and TMC. As the amount of CeO_2 NPs more (0.3-M5), the mechanical stability of the membrane is getting damaged and membrane becomes weakened. The prepared membrane 0.2-M4 with an appropriate amount of CeO_2 NPs improved the membrane's mechanical strength.
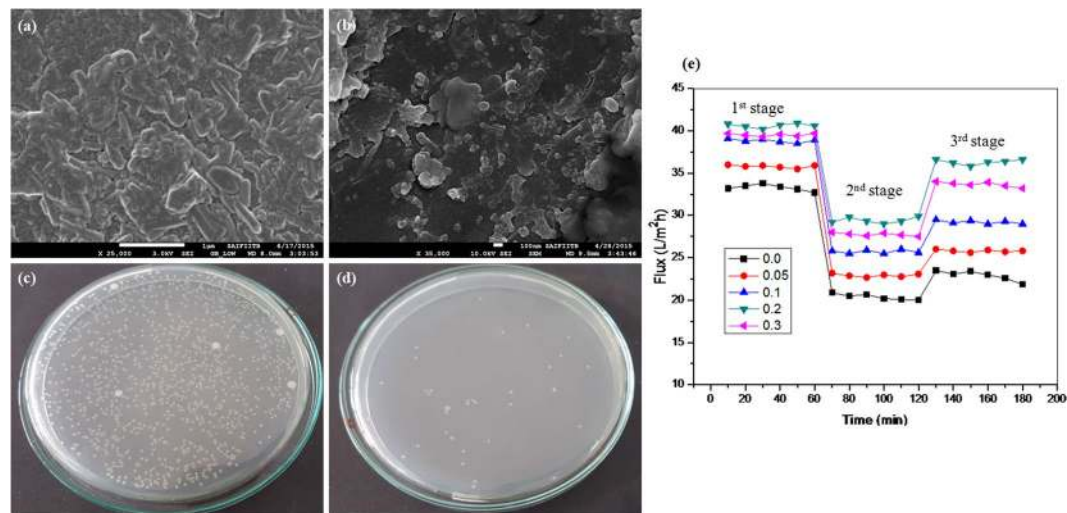
Figure 3. Antibacterial activity by SEM analysis: (**a**) *E. coli* bacteria attached surface morphology of PA membrane and (**b**) CeO$_2$ NPs embedded membranes (incubation for 12 h); digital images observing *E. coli* bacterial culture plates: (**c**) 0-M1 PA (**d**) CeO$_2$ embedded membrane; Flux recovery experiment: (**e**) permeate flux recovery by saltwater (Suvali beach, Surat, India): 1st stage (pure water), 2nd stage (saltwater) and 3rd stage (again pure water).

Anti-bacterial and anti-fouling study.   The anti-bacterial and anti-fouling activity of prepared CeO$_2$-PA TFN membranes is analyzed by using *E. coli* bacteria and saltwater (seawater) (for the composition of saltwater see Table S2), shown in Fig. 3. More fouling resistant, lesser the attachment of foulants and the membrane surface is cleaner.

Anti-bacterial activity of the prepared membrane was analyzed by SEM analysis (Fig. 3a,b) to observe the presence of bacterial cell on the membrane surface. For this analysis membrane was dipped into 5 ml inoculated 10^6 CFU per ml of *E. coli* solution, which is incubated at room temperature. After that membrane was removed from the solution, dried it and take the surface morphology. It shows that the PA membrane (0-M1) is fully covered with the rod-shaped bacterial cell (Fig. 3a), indicating that the membrane has no antibacterial activity compared to CeO$_2$ NPs embedded membrane (0.2-M4), shows the large damage portion of bacterial cells (Fig. 3b) on the surface. The mechanisms can be explained by the fact that the CeO$_2$ NPs is attached to the bacterial cell, causing functional and structural damage and inhibits its growth, leading to the cell death. Anti-bacterial activity is further confirmed by observing the presence of viable cells on Petri plates (Fig. 3c,d). For observing the presence of viable cells, the membrane is dipped into *E. coli* solution, which is also incubated at room temperature. After that, it is moved from the solution, rinsed with normal saline water. The rinse solution is further diluted with distilled water till the concentration became 10^{-3} of the original. Then this diluted solution (0.1 ml) is spread onto the nutrient agar (NA) culture and incubated at 37 °C to observe the viable cells. This result shows that the solution treated with the CeO$_2$ embedded membrane (0.2-M4), shows significantly decreased in a number of colonies (Fig. 3d) as compared with the PA membrane (0-M1) (Fig. 3c). Considering the reasonably low leaching rate (Table S6) at the steady state, the membrane is expected to be effective for long-term for its antibacterial properties due to the strong bonding between the CeO$_2$ NPs and PA thin layer.

Anti-fouling performance is further studied by observing the flux recovery experiment (Fig. 3e) using cross-flow membrane filtration setup (Fig. S5). In Fig. 3e, 1st and 3rd stages are of pure water (0–60 min and 120–180 min) and 2nd stage is of saltwater (60–120 min). In the 1st step, the pure water flux of the CeO$_2$ NPs embedded CeO$_2$-PA TFN membranes (0.05-M2, 0.1-M3, 0.2-M4 and 0.3-M5) is greater than that of the PA membrane (0-M1). The abrupt decline of flux in the 2nd stage is likely due to the increased in osmotic pressure of the saltwater. During the 2nd stage, the PA membrane (0-M1) gets more fouled than in the previous stage. 3rd stage is the recovery of pure water flux, and CeO$_2$-PA TFN membrane (0.2-M4) shows two times higher flux recovery due to the lower fouling. Moreover, the rejection performance of saltwater is also observed on the basis of conductivity, and the results are shown as Fig. S6. Table 3 represents flux recovery ratio (FRR) and flux reduction (FR). It shows that the FRR of 0.2-M4 membrane is higher (86.94%), while 0-M1 membrane shows lesser (66.59%) recovery. Here, high flux recovery of the membrane (0.2-M4) can be credited to its higher hydrophilicity (53.1°), and high surface negativity (−13.34 mC/m^2). An improvement in the hydrophilicity and surface negativity comes out to be an acceptable approach to improve self-cleaning ability to overcome membrane fouling problem. Natural foulants (hydrophobic substance) present in the saltwater has been described as negatively charged substance[23] that is preferred to attach to the positively charged substances. The charge of the natural foulants present in the saltwater (−7.68 mV) is measured using zeta potential measurement.

Salt rejection performance.   The transport phenomena of salts solution through a membrane can be explained by preferential sorption theory. According to this theory, water molecules are sorbs at the membrane

Membranes	Fouling resistant (%)	
	FRR	FR
0-M1	66.59	38.66
0.05-M2	72.06	36.03
0.1-M3	75.48	33.78
0.2-M4	86.94	27.57
0.3-M5	85.3	29.74

Table 3. Fouling resistance of all the modified membranes.
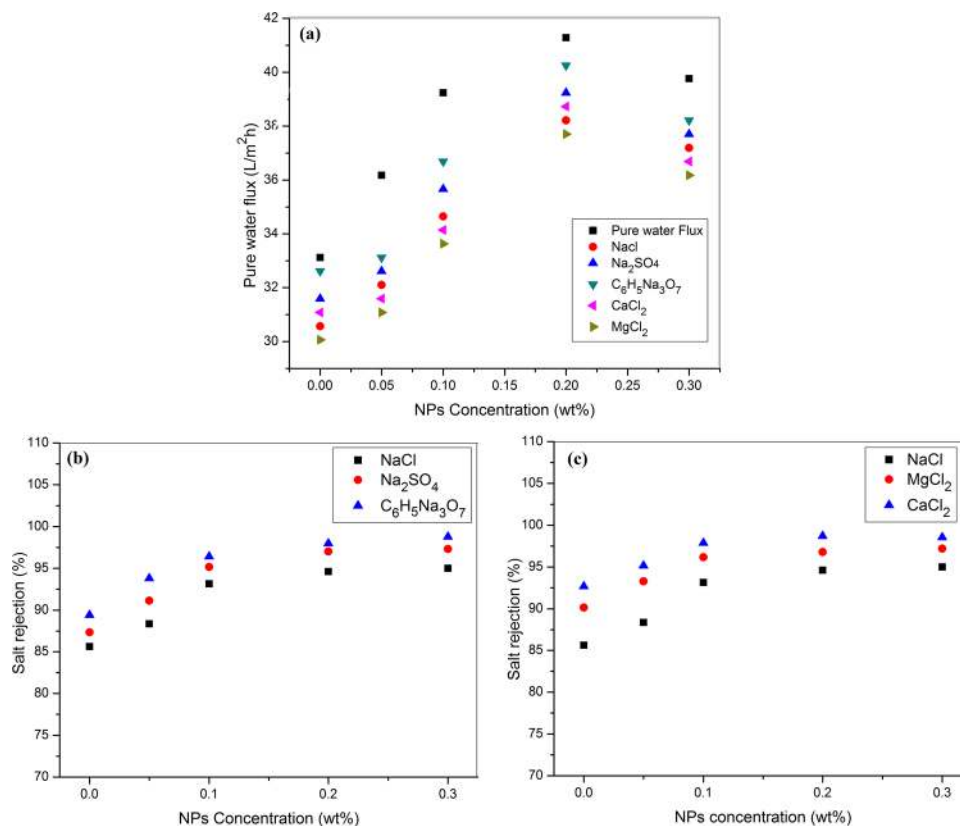
Figure 4. (**a**) Flux of pure and different salt water, salt rejection: (**b**) NaCl, Na_2SO_4 and $C_6H_5Na_3O_7$, and (**c**) NaCl, $CaCl_2$ and $MgCl_2$.

interface and then it moves by a viscous flow through the film in which flux is directly proportional to the pressure. Flux and salt rejection performance of the membranes are shown in the Fig. 4.

The pure water flux increases from 33.12 (0-M1) to 41.28 (0.2-M4) L/m²h with an increase in the concentration of CeO_2 NPs up to 0.2 wt% in CeO_2-PA TFN membranes (Fig. 4a) which show the selectivity of the membrane. The membrane (0.2-M4) prepared with 0.2 wt% of CeO_2 NPs is showed optimal flux, because it increases up to this point, and then decreases with further increases in the concentration of CeO_2 NPs (0.3-M5). This decreasing behavior is caused by the aggregation of NPs, which is occurred more easily at the higher concentration, and again disturbed the dispersion and distribution of CeO_2 NPs into the thin film layer.

The salt rejection follows the order: $C_6H_5Na_3O_7 > Na_2SO_4 > NaCl$ (Fig. 4b) and $CaCl_2 > MgCl_2 > NaCl$ (Fig. 4c). Comparison with the available salt rejection data with NF membrane is given in Table S3. The order of salt rejection (Fig. 4b) is predictable from the Donnan characteristic. CeO_2-PA TFN membrane (0-M1, 0.05-M2, 0.1-M3, 0.2-M4 and 0.3-M5) shows high rejection for low-valence cations and high-valence anions than high-valence cations and low-valence anions ($Na_2SO_4 > NaCl$). It also shows the selectivity of rejection, in which trivalent ions ($C_6H_5Na_3O_7$) showed more rejection than the divalent (Na_2SO_4) and monovalent (NaCl) ions. Because of the number of cations increases, the size of the molecules increases and forms the bulky molecule which does not pass through the CeO_2-PA TFN membrane. Na_2SO_4 is more rejected than NaCl, which is due to the actions of size sieving processes and electrostatic repulsion. Negatively charged (Table 1) surface containing CeO_2-PA TFN membranes shows a strong repulsive force against the divalent (SO_4^{-2}) ions than the monovalent (Cl^-) ions, and prepared CeO_2-PA TFN membranes are negatively charged under the applied pH of 7. Moreover, the radius of SO_4^{-2} (3 Å) ions is bigger than that of Cl^- (1.95 Å) ions[5]. Therefore, SO_4^{-2} ions face more resistance

than Cl^- ions when passing through the CeO_2-PA TFN membrane. The salt rejection is also prohibited by both the charged surface groups present on the outer layer (Fig. S7) that is the most repulsive under some consideration, i.e. by the negatively charged layer (due to the unreacted acid chloride groups) of the surface for multivalent anions (e.g. $C_6H_5Na_3O_7$ and Na_2SO_4) and by the positively charged inner layer (due to the unreacted amines) of the thin layer for multivalent cations ($CaCl_2$, $MgCl_2$, etc.)[39]. Therefore, Ca^{2+} and Mg^{2+} ion (Fig. 4c) has more adsorption ability as compared to Na^+ ion, because positively charged inner layer and thus follows the sequence of rejection $CaCl_2 > MgCl_2 > NaCl$.

Conclusions

This work explains the potential of CeO_2 NPs embedded nanocomposite membrane prepared by pre-seeding interfacial polymerization method for the application of NF process. CeO_2 NPs is added in the different concentration for the preparation of CeO_2-PA TFN NF membrane. Analysis results show the CeO_2 NPs are successfully incorporated in the PA thin layer. CeO_2-PA (0.2-M4) membrane has the higher flux as compared to PA membrane (0-M1). The surface charged of membrane values shows that the addition of CeO_2 NPs increases surface hydrophilicity, as well as surface roughness, decreases. These show that the addition of NPs enhances the wettability of nanocomposite membrane. The new type of CeO_2-PA TFN membranes has the potential to notably improve membrane separation performance and enhancing antibacterial activity against *E. Coli* bacteria. Moreover, as compared to other NPs like silver, CNTs, etc, CeO_2 NPs have a wide range of applications, so there are so many possibilities of this modified nanocomposite membrane for the desalination study in the future research work.

Materials and Methods

Materials. CeO_2 NPs (~50 nm), sodium lauryl sulfate (SLS), m-phenylenediamine (MPD), trimesoyl chloride (TMC), ethanol and hexane were provided by Sigma-Aldrich, India. Polyethersulfone (PES) porous support (75 kDa) was furnished by Permionics Ltd., Baroda. To evaluate the membranes rejection performance, different salts like sodium chloride (NaCl), sodium sulfate (Na_2SO_4), trisodium citrate ($C_6H_5Na_3O_7$), calcium chloride ($CaCl_2$) and magnesium chloride ($MgCl_2$) were purchased by Finar, India. Iodine, barium chloride ($BaCl_2$) and potassium iodide (KI) were provided by Fisher Scientific, India. All the chemicals used in this work were analytical grade mark and used without any purification. PEG (Fisher Scientific, India) with different molecular weights were used for MWCO study to analyze the type of membrane. For membrane anti-fouling activity, nutrient broth (NB), nutrient agar (NA) of Himedia, Mumbai, India, and saltwater of Suvali beach, Surat, India were used. The freeze-dried culture of *E. coli* bacteria was collected from MTCC, IMTECH, Chandigarh. The water used in all the experiments was provided by a Milli-Q system (Millipore Elix, India).

Preparation of CeO_2 NPs embedded nanocomposite membranes. CeO_2 NPs embedded nanocomposite (CeO_2-PA TFN) membranes were prepared on PES porous support by pre-seeding interfacial polymerization method (Fig. S1). In which, first, PES support (diameter: 5.0 cm) was put in an aqueous solution of 0.15 wt% SLS and 2 wt% MPD for 3 min. An excess solution of MPD and SLS were then removed from the surface using tissue paper. A particular amount of CeO_2 NPs (structure, physical and chemical properties of CeO_2 NPs are shown in Table S4) (0–0.3 wt %) were dispersed in an organic phase of hexane and 5 wt% ethanol solution, separately, and subjected to sonication for 5 min. Then, 0.05 wt% of trimesoyl chloride was added to this solution and sonicated for 5 min followed by stirring to get well dispersed pre-assembled CeO_2 NPs. Afterwards, 0.4 ml of this well dispersed pre-assembled sonicated solution was quickly spread on PES support. Spreading was done quickly because of the positive spreading coefficient of hexane solvent. The organic materials that were used to pre-assemble the CeO_2 NPs on a PES support serve here as seeds. The pre-assembled CeO_2 NPs have thus got impregnated with the MPD layer to form a stable, defect-free pre-seeded support. This pre-seeded support was then kept in open air at room temperature to evaporate the extra solution. Afterwards, a solution containing 0.1 wt% TMC and hexane was immediately poured onto the pre-seeded PES support and kept for 1 min for polymerization to take place. After the completion of the reaction, membranes were dried in open air at room temperature and then rinsed with distilled water. Five membranes with different concentration of CeO_2 NPs were prepared (0-M1, 0.05-M2, 0.1-M3, 0.2-M4 and 0.3-M5, wt%) by the same procedure.

Characterization.   Characterization is the first and important step for any prepared/modified membrane to observe its nature, charges, surface chemistry, roughness, pore size, and morphology. A sessile drop manner containing contact angles analysis (Data-Physics OCA15, GmbH, Germany) was used to observe membrane surface nature (hydrophilic or hydrophobic). For that, 1 μL drop of pure water was placed on the dried membrane surface, and the angle was measured with the installed software. The contact angle of buffered and unbuffered electrolytes solution at different pH was also used to calculate the surface charge (using fractional ionization (α), effective acid dissociation constant (pKa) and surface concentration of acidic groups $[COO^-]_o$) of membrane qualitatively by using the Grahame equation[4] (Table S5). To observe surface chemistry and roughness of the membrane, ATR-FTIR (IRAffinity-1S, Shimadzu) and scanning probe microscopy (SPM, Bruker, USA) analysis were used. Prior to these measurements, the samples were desiccated for 24 h to remove moisture. MWCO study was used to observe the pore size of the membrane using PEG with different molecular weights (600, 1000, 1500 Da). 1000 mg/L solution of PEG was used in the cross-flow filtration module and permeates were collected after attaining the steady-state situation. Comparative molecular weights of PEG in permeate and feed were determined using UV spectrophotometer (DR 6000, HACH, USA) at a wavelength of 535 nm against a reagent blank. Iodine, $BaCl_2$, and KI were used for the sample preparation. Membrane morphologies (surface and cross-section) were analyzed under a FEG-SEM instrument by JSM-7600F (JEOL, Japan). Before imaging, membranes were freeze-dried, cracked in liquid nitrogen, and then covered with gold particles. The morphology of PA membrane and CeO_2 NPs embedded membrane were investigated using a TEM CM 200 instrument (Philips). The

mechanical properties (tensile strength and elongation) of membranes were tested by a tensile testing machine (Tensometer, Kudale PC-2000). The membrane samples were cut into pieces in a particular shape with a total length of 10 cm and width of 1.5 cm and then dried it. The cross head speed was maintaining 20 mm/min.

Membrane performance. Anti-bio-fouling property of the CeO_2-PA TFN membrane was analyzed by measuring the growth status of microbial cells on the membrane surface. *E. coli* bacteria were inoculated in the 5 ml of NB solution for 12 h at 37 °C. The membrane (0.03 g) was measured, cut and sterilized for 20 min, respectively. To analyze the antibacterial property, membrane sample was added to 5 ml inoculated 10^6 CFU per ml of *E. coli* solution, which was incubated at room temperature. After 24 h, the sample was removed from the culture and rinsed with normal saline water. The rinse solution was collected and further diluted with distilled water till the concentration became 10^{-3} of the original. Then the diluted solution (0.1 ml) was spread onto the NA culture and the Petri plates were incubated at 37 °C for 24 h to observe the growth status of microbial cells.

Anti-fouling performance of the CeO_2-PA TFN membranes was studied by performing flux recovery experiment using saltwater collected from the Suvali beach according to the following steps: (i) pure water flux, (ii) filtration of saltwater solution is performed and flux is measured, (iii) washing with pure water and (iv) again pure water flux is measured. A laboratory-made cross-flow membrane filtration setup was used for all the experiments, in which four stainless steel modules attached in series. The membrane modules were possessed space to put flat-sheet circular membrane part with an area of 18.85 cm². A reciprocating diaphragm type pump (model no.: mROY B-13) was used to pass the feed solution through the membrane. The valve sited at the end of the module was used to pressurize the feed and control the feed pressure. All membranes were initially compressed at 200 psi pressure until steady-state flow was achieved. Flux (J) of pure water and salt solution, different salt rejection (%) experiments, flux recovery ratio (FRR) and flux reduction (FR) of the membranes were carried out at operating pressure 300 psi. Flux, FRR, and FR of the membrane can be calculated using equations (1), (2) and (3) as shown below.

$$J = \frac{V_p}{A \times t} \tag{1}$$

$$FRR(\%) = \frac{J_{w2}}{J_{w1}} \times 100 \tag{2}$$

$$FR(\%) = \left(1 - \frac{J_f}{J_{w1}}\right) \times 100 \tag{3}$$

where, J: the flux (L/m²h), A: the membrane area (m²), V_p: the permeate volume (ml) and t: treatment time (h). J_{w1}: the average pure water flux during the first stage, J_f: the feed flux (saltwater) solution and J_{w2}: the average of pure water flux during the third stage.

The salt rejection performance of the membranes was observed by filtering NaCl, Na_2SO_4, $C_6H_5Na_3O_7$, $CaCl_2$, and $MgCl_2$ salts solution at an initial concentration of 2000 mg/L. The conductivity of solutions (feed and permeate) was measured by a conductivity meter connected to the system, and a calibration curve was used to relate the solution conductivity to salt concentration. The salt rejection, R, was calculated from the equation (4) as shown below:

$$R(\%) = \left(1 - \frac{c_p}{c_f}\right) \times 100 \tag{4}$$

where C_p: the conductivity of salt in permeates and C_f: the conductivity of salt in feed solutions.

Leaching Test: The leaching rate of cerium ions from CeO_2 NPs embedded TFN membrane was examined by the cerium stability experiments. So, first CeO_2 NPs embedded TFN membrane was cut into a particular shape with an area 1 cm² and was subsequently immersed in 20 ml of pure water at room temperature for 2, 4 and 24 h. After determined time frames, the amount of cerium ion in the water was analyzed by UV spectrophotometer.

References

1. Yu, H. Y. *et al.* Surface modification of polypropylene microporous membrane to improve its antifouling property in MBR: CO_2 plasma treatment. *J. Membr. Sci.* **254**, 219–227 (2005).
2. Prince, J. A., Bhuvana, S., Boodhoo, K. V. K., Anbharasi, V. & Singh, G. Synthesis and characterization of PEG-Ag immobilized PES hollow fiber ultrafiltration membranes with long lasting antifouling properties. *J. Membr. Sci.* **454**, 538–548 (2014).
3. Heidi Lynn, R., Priscilla, G. L. B. & Emmanuel, I. Metal nanoparticle modified polysulfone membranes for use in wastewater treatment: a critical review. *JSEMAT* **2**, 183–193 (2012).
4. Hurwitz, G., Guillen, G. R. & Hoek, E. M. Probing polyamide membrane surface charge, zeta potential, wettability, and hydrophilicity with contact angle measurements. *J. Membr. Sci.* **349**, 349–357 (2010).
5. Yin, J., Kim, E. S., Yang, J. & Deng, B. Fabrication of a novel thin-film nanocomposite (TFN) membrane containing MCM-41 silica nanoparticles (NPs) for water purification. *J. Membr. Sci.* **423**, 238–246 (2012).
6. Rajaeian, B., Rahimpour, A., Tade, M. O. & Liu, S. Fabrication and characterization of polyamide thin film nanocomposite (TFN) nanofiltration membrane impregnated with TiO_2 nanoparticles. *Desalination* **313**, 176–188 (2013).
7. Heo, J. *et al.* Highly Permeable Graphene Oxide/Polyelectrolytes Hybrid Thin Films for Enhanced CO_2/N_2 Separation Performance. *Sci. Rep.* **7**, 456 (2017).
8. Yin, J. & Deng, B. Polymer-matrix nanocomposite membranes for water treatment. *J. Membr. Sci.* **479**, 256–275 (2015).
9. Goh, P. S., Ng, B. C., Lau, W. J. & Ismail, A. F. Inorganic nanomaterials in polymeric ultrafiltration membranes for water treatment. *Sep. Purif. Rev.* **44**, 216–249 (2015).

10. Homayoonfal, M. *et al.* A comparison between blending and surface deposition methods for the preparation of iron oxide/polysulfone nanocomposite membranes. *Desalination* **354**, 125–142 (2014).
11. Mo, J., Son, S. H., Jegal, J., Kim, J. & Lee, Y. H. Preparation and characterization of polyamide nanofiltration composite membranes with TiO$_2$ layers chemically connected to the membrane surface. *J. Appl. Polym. Sci.* **105**, 1267–1274 (2007).
12. Wu, H., Tang, B. & Wu, P. MWNTs/polyester thin film nanocomposite membrane: an approach to overcome the trade-off effect between permeability and selectivity. *J. Phys. Chem. C Nanomater. Interfaces.* **114**, 16395 (2010).
13. Lau, W. J. *et al.* A review on polyamide thin film nanocomposite (TFN) membranes: history, applications, challenges and approaches. *Water Res.* **80**, 306–324 (2015).
14. Luo, M. L., Zhao, J. Q., Tang, W. & Pu, C. S. Hydrophilic modification of poly (ether sulfone) ultrafiltration membrane surface by self-assembly of TiO$_2$ nanoparticles. *Appl. Surf. Sci.* **249**, 76–84 (2005).
15. Nguyen, A., Zou, L. & Priest, C. Evaluating the antifouling effects of silver nanoparticles regenerated by TiO$_2$ on forward osmosis membrane. *J. Membr. Sci.* **454**, 264–271 (2014).
16. Huang, H., Qu, X., Dong, H., Zhang, L. & Chen, H. Role of NaA zeolites in the interfacial polymerization process towards a polyamide nanocomposite reverse osmosis membrane. *RSC Adv.* **3**, 8203–8207 (2013).
17. Lind, M. L., Eumine Suk, D., Nguyen, T. V. & Hoek, E. M. Tailoring the structure of thin film nanocomposite membranes to achieve seawater RO membrane performance. *Environ. Sci. Technol.* **44**, 8230–8235 (2010).
18. Kim, S. G., Hyeon, D. H., Chun, J. H., Chun, B. H. & Kim, S. H. Nanocomposite poly (arylene ether sulfone) reverse osmosis membrane containing functional zeolite nanoparticles for seawater desalination. *J. Membr. Sci.* **443**, 10–18 (2013).
19. Bao, M., Zhu, G., Wang, L., Wang, M. & Gao, C. Preparation of monodispersed spherical mesoporous nanosilica–polyamide thin film composite reverse osmosis membranes via interfacial polymerization. *Desalination* **309**, 261–266 (2013).
20. Kim, E. S., Hwang, G., El-Din, M. G. & Liu, Y. Development of nanosilver and multi-walled carbon nanotubes thin-film nanocomposite membrane for enhanced water treatment. *J. Membr. Sci.* **394**, 37–48 (2012).
21. Lee, S. Y. *et al.* Silver nanoparticles immobilized on thin film composite polyamide membrane: characterization, nanofiltration, antifouling properties. *Polym. Adv. Technol.* **18**, 562–568 (2007).
22. Rana, D. & Matsuura, T. Surface modifications for antifouling membranes. *Chem. Rrev.* **110**, 2448–2471 (2010).
23. Kim, E. S., Liu, Y. & El-Din, M. G. An *in-situ* integrated system of carbon nanotubes nanocomposite membrane for oil sands process-affected water treatment. *J. Membr. Sci.* **429**, 418–427 (2013).
24. Wu, H., Tang, B. & Wu, P. Development of novel SiO$_2$–GO nanohybrid/polysulfone membrane with enhanced performance. *J. Membr. Sci.* **451**, 94–102 (2014).
25. Duan, L., Zhao, Q., Liu, J. & Zhang, Y. Antibacterial behavior of halloysite nanotubes decorated with copper nanoparticles in a novel mixed matrix membrane for water purification. Environ. *Sci.: Water Res. Technol.* **1**, 874–881 (2015).
26. Krishnamoorthy, K., Veerapandian, M., Zhang, L. H., Yun, K. & Kim, S. J. Surface chemistry of cerium oxide nanocubes: Toxicity against pathogenic bacteria and their mechanistic study. *J. Ind. Eng. Chem.* **20**, 3513–3517 (2014).
27. Dahle, J. T. & Arai, Y. Environmental geochemistry of cerium: applications and toxicology of cerium oxide nanoparticles. *Int. J. Environ. Res. Public Health* **12**, 1253–1278 (2015).
28. Gu, H. & Soucek, M. D. Preparation and characterization of monodisperse cerium oxide nanoparticles in hydrocarbon solvents. *Chem. Mater.* **19**, 1103–1110 (2007).
29. Pelletier, D. A. *et al.* Effects of engineered cerium oxide nanoparticles on bacterial growth and viability. *Appl. Environ. Microbiol.* **76**, 7981–7989 (2010).
30. Thill, A. *et al.* Cytoanti-bacterial activity of CeO$_2$ NPs for Escherichia coli. Physico-chemical insight of the cytoanti-bacterial activity mechanism. *Environ. Sci. Technol.* **40**, 6151–6156 (2006).
31. Fang, X., Yu, R., Li, B., Somasundaran, P. & Chandran, K. Stresses exerted by ZnO, CeO$_2$ and anatase TiO$_2$ nanoparticles on the Nitrosomonas europaea. *J. Colloid Interface Sci.* **348**, 329–334 (2010).
32. Peng, X. *et al.* Ceria nanoparticles supported on carbon nanotubes for the removal of arsenate from water. *Mater. Lett.* **59**, 399–403 (2005).
33. Di, Z. C. *et al.* Chromium adsorption by aligned carbon nanotubes supported ceria nanoparticles. *Chemosphere* **62**, 861–865 (2006).
34. Kim, J. & der Bruggen, V. B. The use of nanoparticles in polymeric and ceramic membrane structures: review of manufacturing procedures and performance improvement for water treatment. *Environ. Pollut.* **158**, 2335–2349 (2010).
35. Lu, H. *et al* An overview of nanomaterials for water and wastewater treatment. *Adv. Mater. Sci. Eng.* **2016** (2016).
36. Krishnamoorthy, K., Veerapandian, M., Zhang, L. H., Yun, K. & Kim, S. J. Antibacterial efficiency of graphene nanosheets against pathogenic bacteria via lipid peroxidation. *The J. Phys. Chem. C* **116**, 17280–17287 (2012).
37. Lau, W. J. *et al.* A review on polyamide thin film nanocomposite (TFN) membranes: History, applications, challenges and approaches. *Water Res.* **80**, 306–324 (2015).
38. Kong, C., Shintani, T. & Tsuru, T. "Pre-seeding"-assisted synthesis of a high performance polyamide-zeolite nanocomposite membrane for water purification. *New J. Chem.* **34**, 2101–2104 (2010).
39. Zhu, H., Szymczyk, A. & Balannec, B. On the salt rejection properties of nanofiltration polyamide membranes formed by interfacial polymerization. *J. Membr. Sci.* **379**, 215–223 (2011).

Acknowledgements

Author Contributions

Mausumi Mukhopadhyay conceptualized the research work and supervised the work done all through with details contribution in discussing and reviewing the manuscript with technical inputs. Sonia R. Lakhotia as part of her PhD research performed all the experiments, characterization, and test, calculation, drawn Figures 1, S1, S5, S6 and data analysis of all results and wrote the manuscript. Premlata Kumari helped Sonia R. Lakhotia in some analysis and reviewed her work.

Additional Information